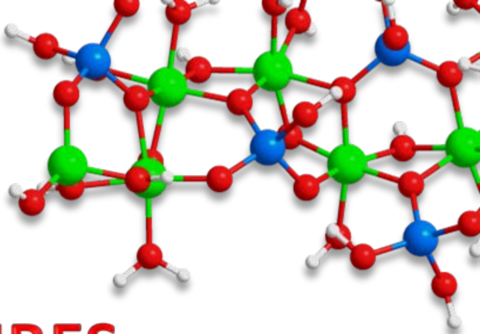

FORMATION and GROWTH MECHANISMS of SINGLE-WALLED METAL OXIDE NANOTUBES

IPEK YUCELEN
GEORGIA INSTITUTE of TECHNOLOGY
School of Materials Science and Engineering
Nano@Tech

ADVISERS: Prof. SANKAR NAIR
School of Chemical & Biomolecular Engineering

Prof. HASKELL W. BECKHAM
School of Materials Science and Engineering

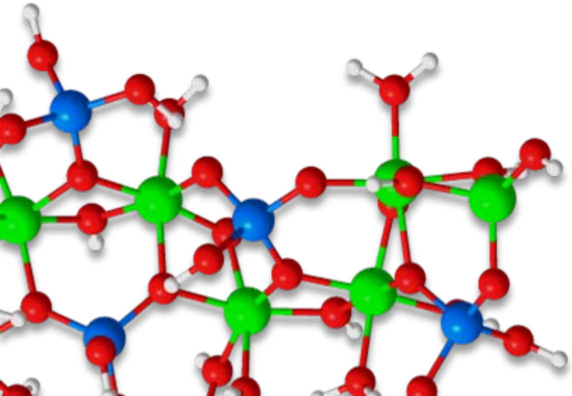

Single-Walled Metal Oxide Nanotubes

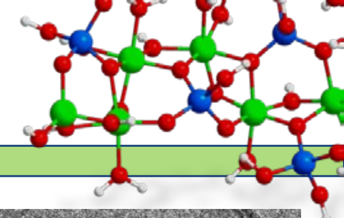

Ball-and-stick models of (left) the **aluminosilicate nanotube**, and (right) a section of the wall showing the hexagonal aluminosilicate repeat units.

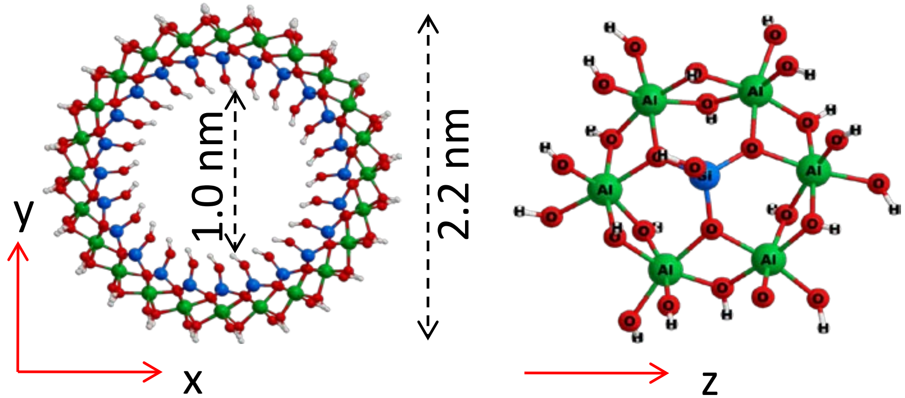

- Aluminum hydroxide shell $[(OH)_3Al_2]$
- Interior silanol groups $[O_3SiOH]$
- Average length ~ 100 nm
- Offers a vast range of compositions and dimensions

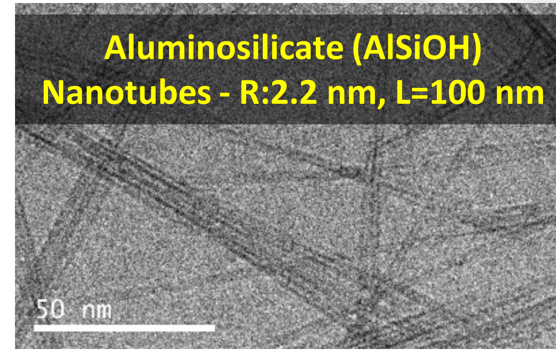

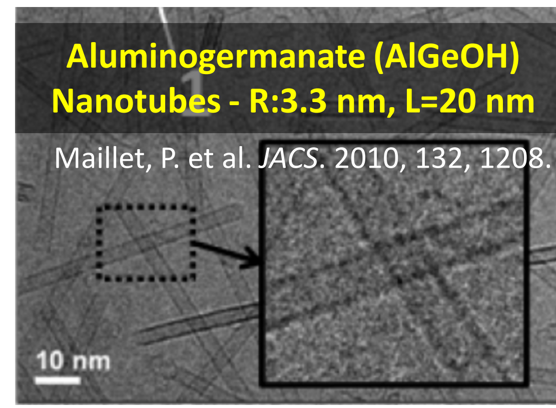

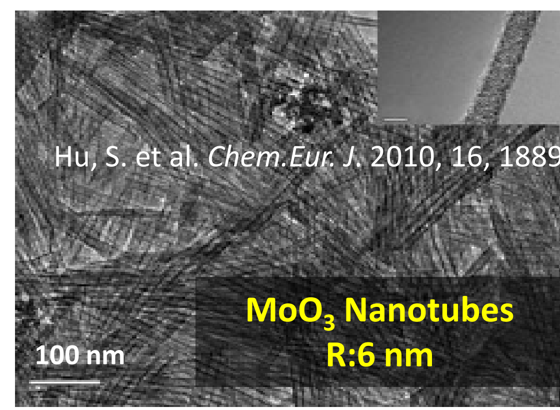

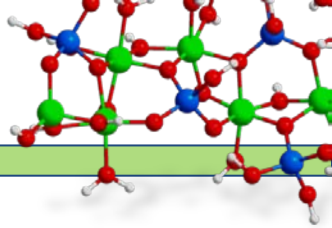

Applications of Single-Walled Metal Oxide Nanotubes

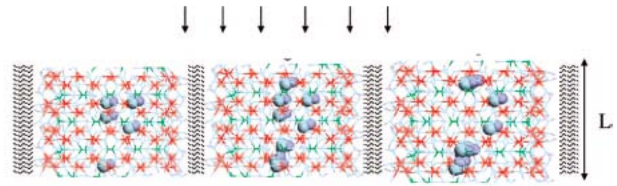

Nanofluidic Membranes

Konduri, S., et al. *J. Phys. Chem. C*, 2008, 112, 15367.
Zang, J., et al. *ACS Nano*, 2009, 3, 1548.

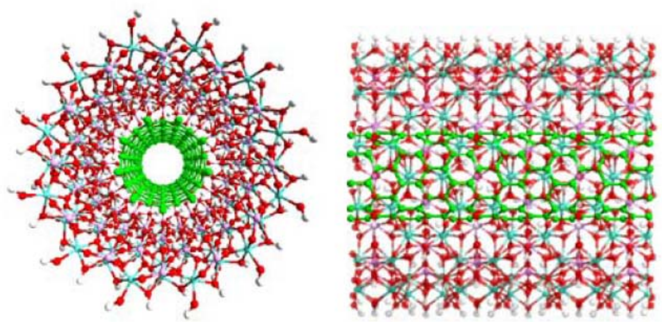

Nanocables

Kuc, A. and T. Heine, *Advanced Materials*, 2009, 21, 4353.

Kang, D.-Y., et al. *J. Phys. Chem. C*, 2011, 115, 7676.

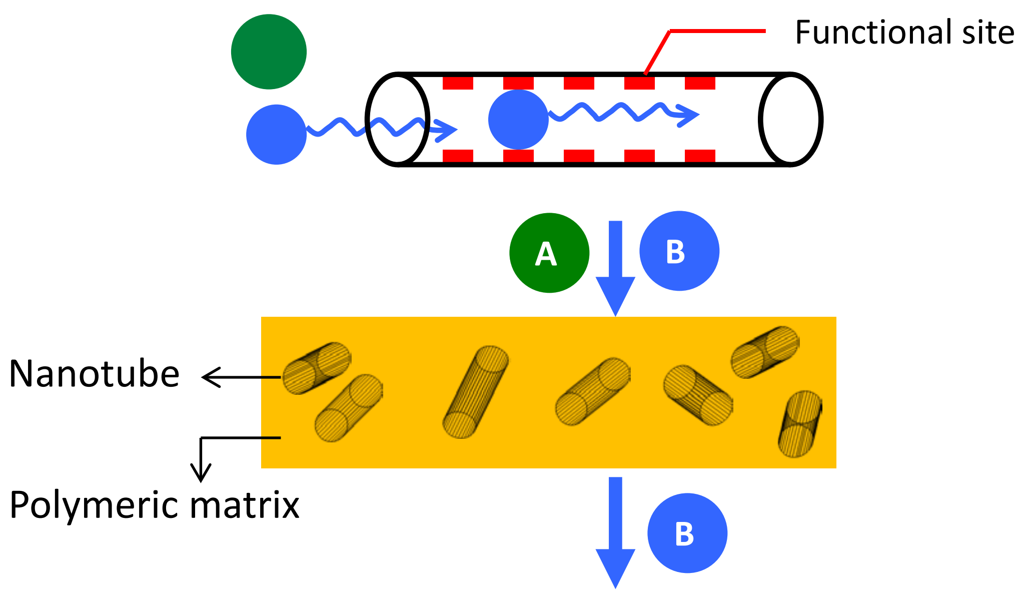

Molecular Separations

Kang, D.-Y., et al. *ACS Applied Materials & Interfaces*, 2012, 4, 965.
Kang, D.-Y., et al. *Journal of Membrane Science*, 2011, 381, 50.
Zang, J., et al. *J. Phys. Chem. Lett.*, 2010, 1, 1235.

Synthesis of Single-Walled Metal Oxide Nanotubes

- Low temperatures synthesis (95°C)
- Inexpensive and easily accessible reactants
- Can be obtained in pure form

Al - Aluminum-tri-*sec*-butoxide (ASB) **+**
Si - Tetraethyl orthosilicate (TEOS) in $HClO_4$

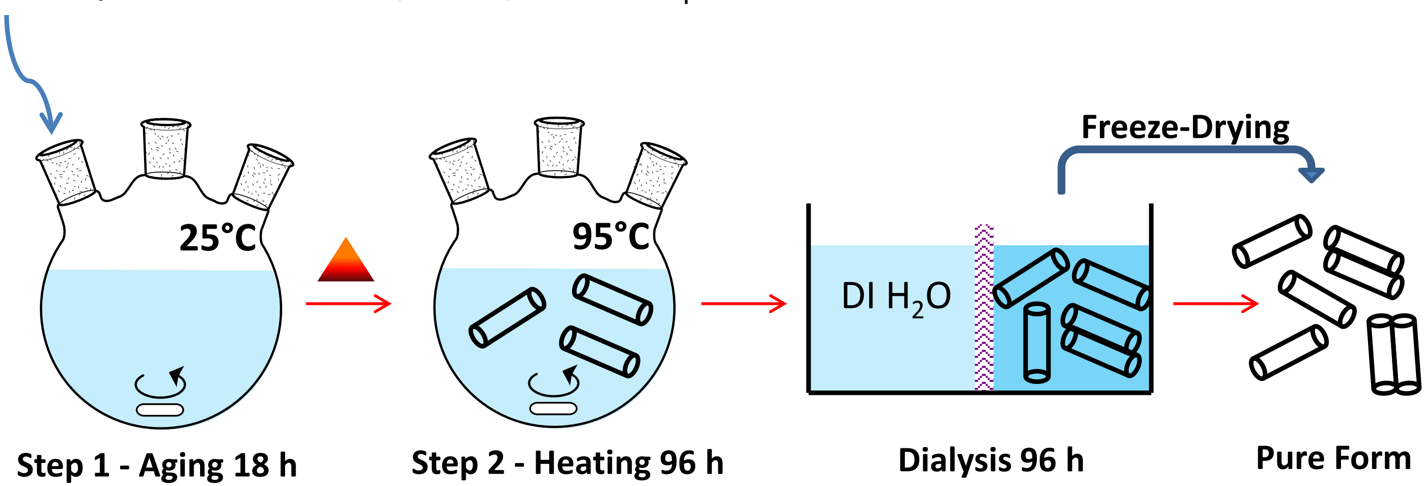

Research Objectives

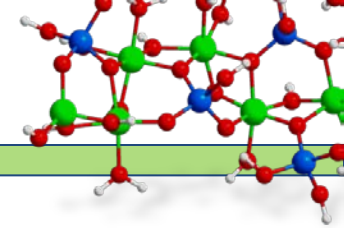

Engineering inorganic nanoscopic objects

Ångstrom Level
Dimensional *Control*

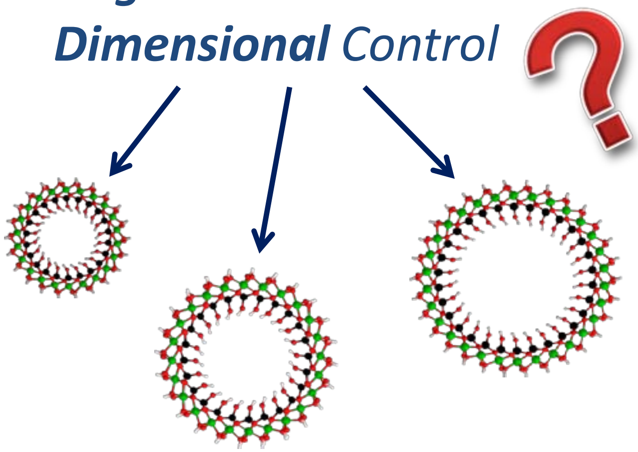

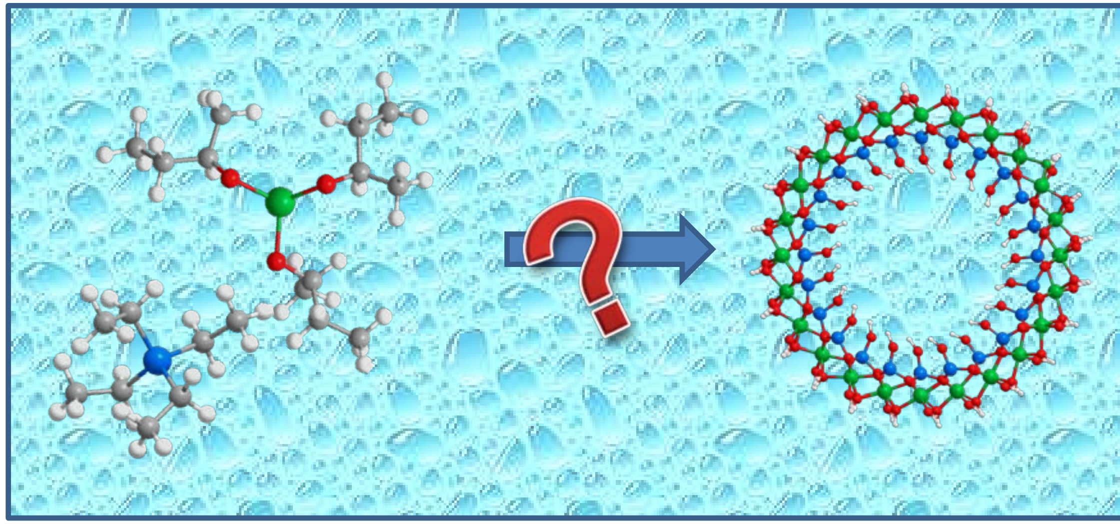

- Exemplary material – aluminosilicate nanotubes
- Identification of nanointermediates and local structural evolution – Nuclear Magnetic Resonance (NMR), Electrospray Ionization Mass Spectrometry (ESI-MS)
- Molecular Configuration – solvated Density Functional Theory (DFT) simulations
- Structural characterization at larger scales – Cryo-electron Microscopy, and TEM

Aluminosilicate Speciation During Aging (25˚C) – ESI-MS

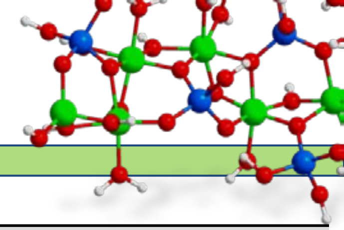

- $Al_1Si_X(ClO_4)_y$ – $Al_{13}Si_x(ClO_4)_y$ (x= 0-7, y= 0-5)
- Complete and incomplete Al_6Si ring units
- Speciation is same throughout the aging

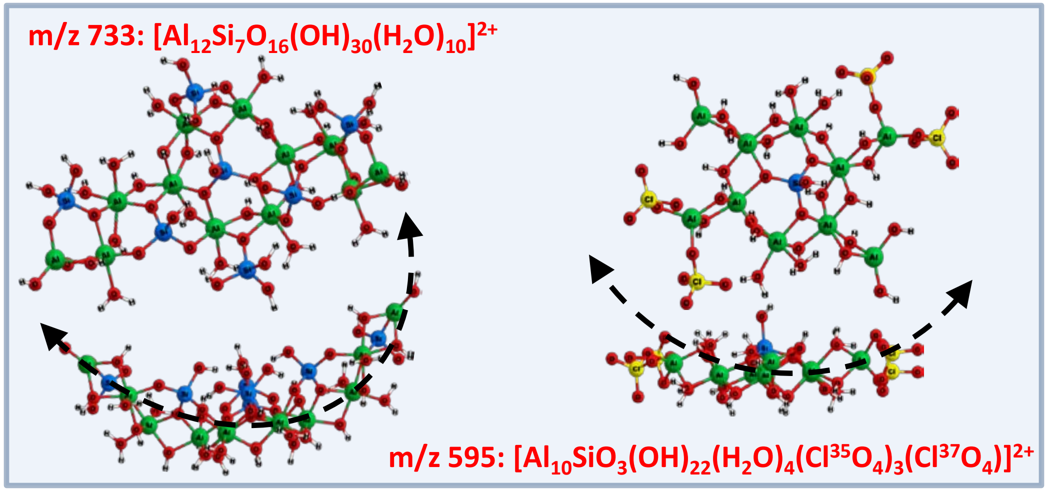

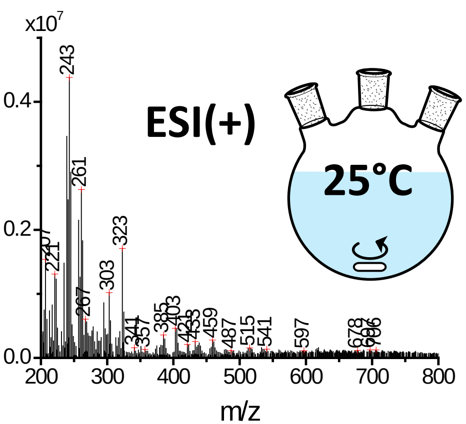

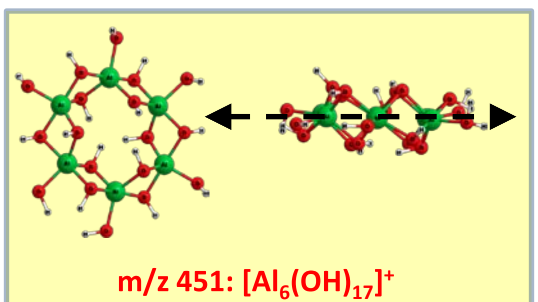

Chemical Formula of AlSi Species	Peak Series (m/z)
$[Al(OH)_2(H_2O)_n]^+$	61+18n (n=0-2)
$[Al(OH)(H_2O)_n(ClO_4)]^+$	143+18n (n=0-3)
$[Al(H_2O)_n(ClO_4)_2]^+$	225+18n (n=0-3)
$[Al_2(OH)_5(H_2O)_n]^+$	139+18n (n=0-2)
$[Al_2(OH)_4(ClO_4)(H_2O)_n]^+$	221+18n (n=0-3)
$[Al_2SiO_2(OH)_5(H_2O)_{n+1}]^+$	217+18n (n=0-3)
$[Al_3SiO_2(OH)_6(H_2O)_n(ClO_4)]^{2+}$	171+9n (n=0-5)
$[Al_3SiO_2(OH)_8(H_2O)_n]^+$	277+18n (n=0-2)
$[Al_7Si_2O_5(OH)_{13}(H_2O)_{n+3}(ClO_4)_3]^{3+}$	299+6n (n=0-4)
$[Al_2(OH)_3(H_2O)_n(ClO_4)_2]^+$	303+18n (n=0-5)
$[Al_7Si_2O_5(OH)_{12}(H_2O)_n(Cl^{35}O_4)_3(Cl^{37}O_4)]^{3+}$	309+6n (n=0-10)
$[Al_8Si_2O_6(OH)_{13}(H_2O)_n(Cl^{35}O_4)_3(Cl^{37}O_4)]^{3+}$	329+6n (n=0-7)
$[Al_2(OH)_2(H_2O)_n(ClO_4)_3]^+$	385+18n (n=0-4)
$[Al_2(OH)_2(H_2O)_n(Cl^{35}O_4)_2(Cl^{37}O_4)]^+$	387+18n (n=0-4)
$[Al_2SiO(OH)_5(H_2O)_n(ClO_4)_2]^+$	381+18n (n=0-3)
$[Al_4SiO_3(OH)_8(H_2O)_{n+1}(ClO_4)]^+$	437+18n (n=0-2)
$[Al_2SiO(OH)_4(H_2O)_n(ClO_4)_3]^+$	463+18n (n=0-4)
$[Al_5SiO_3(OH)_{12}(H_2O)_{n+1}]^+$ / $[Al_4Si_2O_4(OH)_{11}(H_2O)_{n+1}]^+$	433+18n (n=0-6)
$[Al_5Si_2O_5(OH)_{12}(H_2O)_{n+1}]^+$	493+18n (n=0-3)
$[Al_6SiO_3(OH)_{15}(H_2O)_n]^+$	493+18n (n=0-3)
$[Al_4Si_2O_4(OH)_{10}(H_2O)_n(ClO_4)]^+$	497+18n (n=0-4)
$[Al_{10}SiO_3(OH)_{22}(H_2O)_n(ClO_4)_3(ClO_4)]^{2+}$	559+9n (n=0-4)
$[Al_8Si_2O_5(OH)_{15}(H_2O)_{n+5}(Cl^{35}O_4)_4(Cl^{37}O_4)]^{2+}$	597+9n (n=0-4)
$[Al_{10}Si_3O_9(OH)_{18}(H_2O)_{n+1}(Cl^{35}O_4)_3(Cl^{37}O_4)]^{2+}$	610+9n (n=0-5)
$[Al_{12}Si_3O_9(OH)_{27}(H_2O)_{n+6}(Cl^{35}O_4)]^{2+}$	609+9n (n=0-4)
$[Al_{12}Si_3O_9(OH)_{25}(H_2O)_n(Cl^{35}O_4)_2(Cl^{37}O_4)]^{2+}$	638+9n (n=0-6)
$[Al_{13}Si_2O_{10}(OH)_{22}(H_2O)_{n+1}(Cl^{35}O_4)_2(Cl^{37}O_4)]^{2+}$	638+9n (n=0-6)
$[Al_{12}Si_3O_9(OH)_{26}(H_2O)_{n+1}(ClO_4)_2]^{2+}$	605+9n (n=0-7)
$[Al_{12}Si_5O_{12}(OH)_{29}(H_2O)_{n+3}(ClO_4)]^{2+}$	678+9n (n=0-4)
$[Al_{13}O_4(OH)_{24}(H_2O)_{n+2}(Cl^{35}O_4)_4(Cl^{37}O_4)]^{2+}$	678+9n (n=0-4)
$[Al_{12}Si_4O_{10}(OH)_{29}(H_2O)_{n+6}(Cl^{35}O_4)]^{2+}$	648+9n (n=0-4)
$[Al_{12}Si_7O_{16}(OH)_{30}(H_2O)_{n+5}]^{2+}$	688+9n (n=0-5)
$[Al_{12}Si_4O_{10}(OH)_{28}(H_2O)_{n+8}(Cl^{35}O_4)_2]^{2+}$	707+9n (n=0-4)
$[Al_{13}Si_4O_{16}(OH)_{18}(H_2O)_{n+5}(Cl^{35}O_4)_2(Cl^{37}O_4)]^{2+}$	707+9n (n=0-4)
$[Al_{12}Si_7O_{13}(OH)_{35}(H_2O)_{n+5}(ClO_4)]^{2+}$	756+9n (n=0-3)
$[Al_{13}Si_6O_{10}(OH)_{40}(H_2O)_{n+3}(ClO_4)]^{2+}$	756+9n (n=0-3)

Aluminosilicate Speciation During Aging (95˚C) – ESI-MS

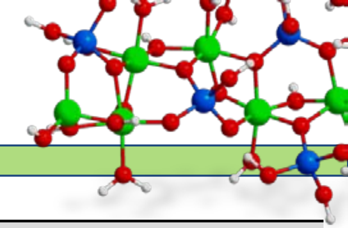

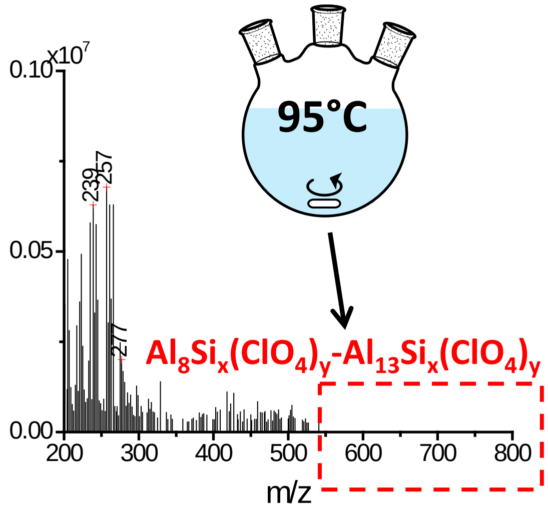

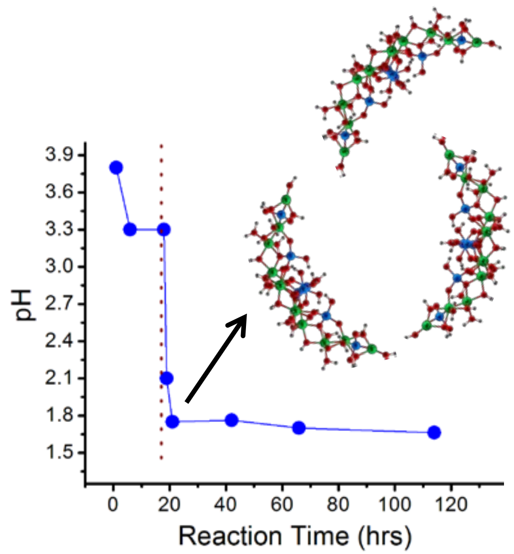

Chemical Formula of AlSi Species	Peak Series m/z
$[Al(OH)_2(H_2O)_n]^+$	61+18n (n=0-2)
$[Al(OH)(H_2O)_n(ClO_4)]^+$	143+18n (n=0-3)
$[Al(H_2O)_n(ClO_4)_2]^+$	225+18n (n=0-3)
$[Al_2(OH)_5(H_2O)_n]^+$	139+18n (n=0-2)
$[Al_2(OH)_4(ClO_4)(H_2O)_n]^+$	221+18n (n=0-3)
$[Al_2SiO_2(OH)_5(H_2O)_{n+1}]^+$	217+18n (n=0-3)
$[Al_3SiO_2(OH)_6(H_2O)_n(ClO_4)]^{2+}$	171+9n (n=0-5)
$[Al_3SiO_2(OH)_8(H_2O)_n]^+$	277+18n (n=0-2)
$[Al_7Si_2O_5(OH)_{13}(H_2O)_{n+3}(ClO_4)_3]^{3+}$	299+6n (n=0-4)
$[Al_2(OH)_3(H_2O)_n(ClO_4)_2]^+$	303+18n (n=0-5)
$[Al_7Si_2O_5(OH)_{12}(H_2O)_n(Cl^{35}O_4)_3(Cl^{37}O_4)]^{3+}$	309+6n (n=0-10)
$[Al_2(OH)_2(H_2O)_n(ClO_4)_3]^+$	385+18n (n=0-4)
$[Al_2(OH)_2(H_2O)_n(Cl^{35}O_4)_2(Cl^{37}O_4)]^+$	387+18n (n=0-4)
$[Al_2SiO(OH)_5(H_2O)_n(ClO_4)_2]^+$	381+18n (n=0-3)
$[Al_4SiO_3(OH)_8(H_2O)_{n+1}(ClO_4)]^+$	437+18n (n=0-2)
$[Al_2SiO(OH)_4(H_2O)_n(ClO_4)_3]^+$	463+18n (n=0-4)
$[Al_5SiO_3(OH)_{12}(H_2O)_{n+1}]^+$	433+18n (n=0-6)
$[Al_5Si_2O_5(OH)_{12}(H_2O)_{n+1}]^+$	493+18n (n=0-3)
$[Al_6SiO_3(OH)_{15}(H_2O)_n]^+$	493+18n (n=0-3)
$[Al_4Si_2O_4(OH)_{10}(H_2O)_n(ClO_4)]^+$	497+18n (n=0-4)
$[Al_3SiO_2(OH)_7(H_2O)_{n+6}]^{2+}$	184+9n (n=0-1)
$[Al_3SiO_2(OH)_5(H_2O)_{n+6}(ClO_4)_2]^{2+}$	266+9n (n=0-1)
$[Al_3SiO_2(OH)_8(H_2O)_{n+2}]^+$	313+18n (n=0-2)

- $Al_1Si_x(ClO_4)_y$ – $Al_7Si_x(ClO_4)_y$ (x= 0-2, y= 0-3)
- Nanotube-like intermediates (*m/z* 500-800) disappear from ESI-MS spectra
- Abrupt pH drop from 3.3 to 1.7 upon heating to 95 ˚C
- Condensation of curved nano-intermediates takes place

^{27}Al Liquid-State NMR

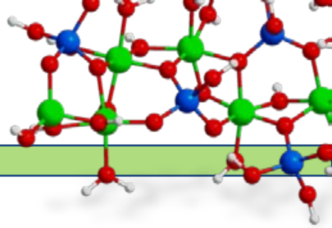

Nanotube-like Hexa-coordination

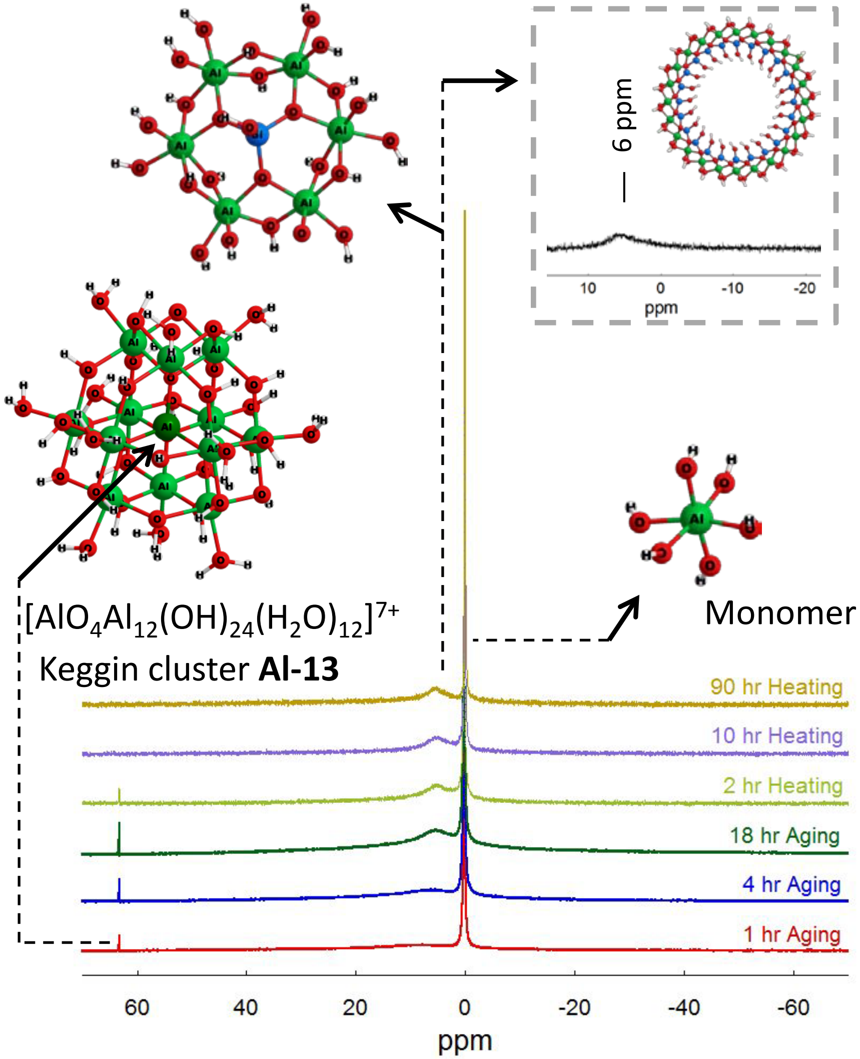

- Keggin cluster **Al-13** (63.3 ppm, 12 ppm)
- Hexa-coordinated monomer **Al-1** (0 ppm)
- Nanotube-like hexa-coordination (~6 ppm)

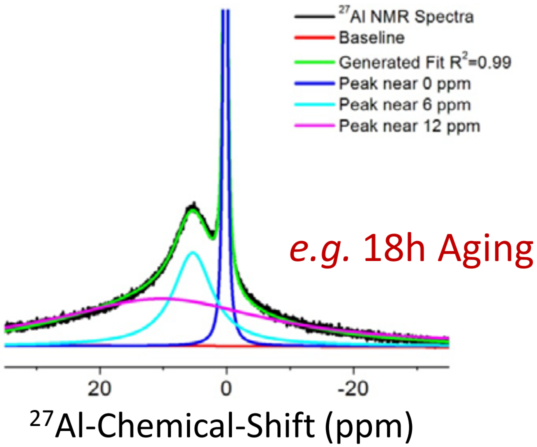

- Nanotube-like and Keggin species
- Chemical shift, linewidth and integrated areas of each peak are examined

^{27}Al Liquid-State NMR

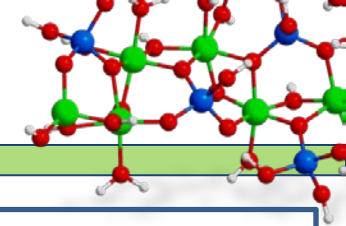

- Area of NMR resonances — concentration in solution

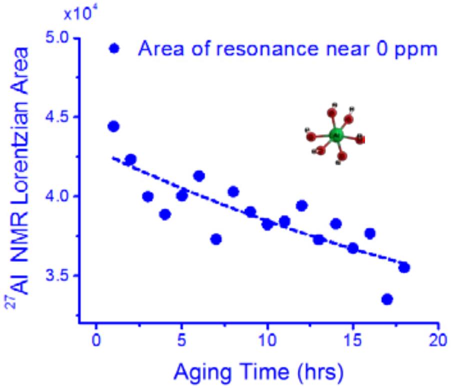

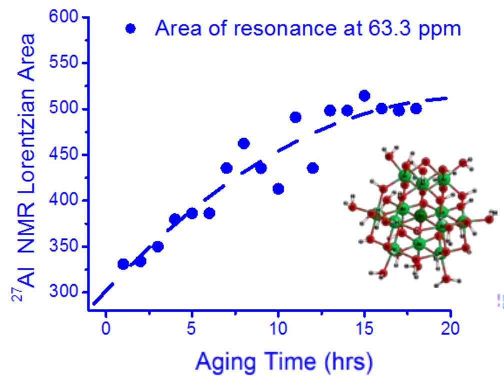

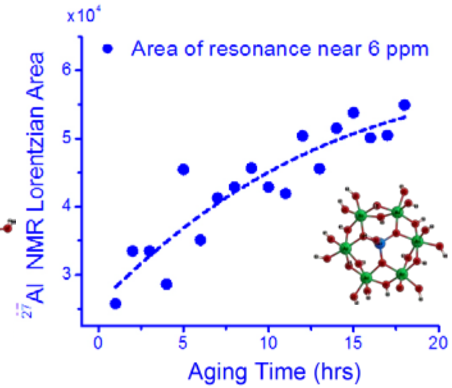

Aging Stage at 25˚C

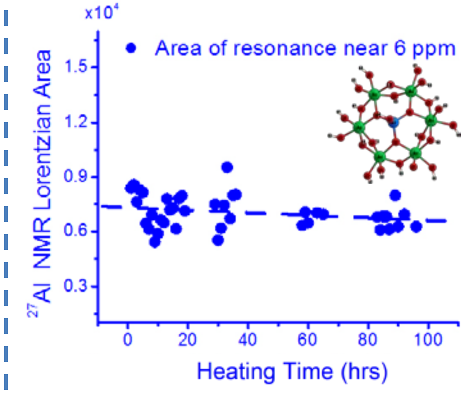

Heating Stage at 95˚C

- FWHM (full width at half maximum) —environmental ordering around Al

Aging Stage at 25˚C

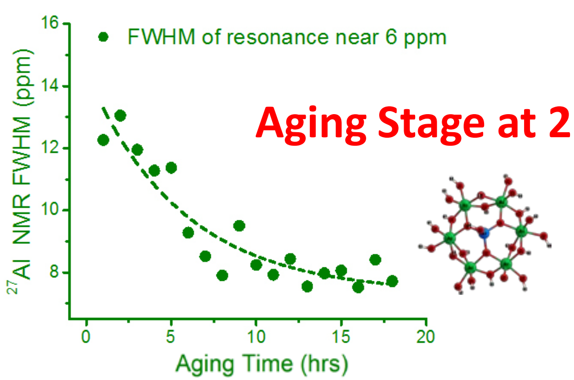

- Chemical shift — structure

Heating Stage at 95˚C

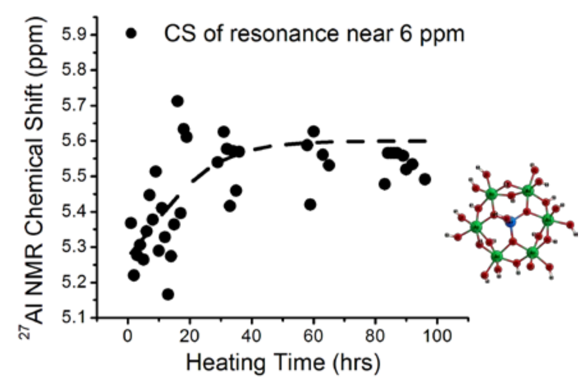

Overall Mechanism of Nanotube Formation

Formation of Single-Walled Aluminosilicate Nanotubes from Molecular Precursors and Curved Nanoscale Intermediates

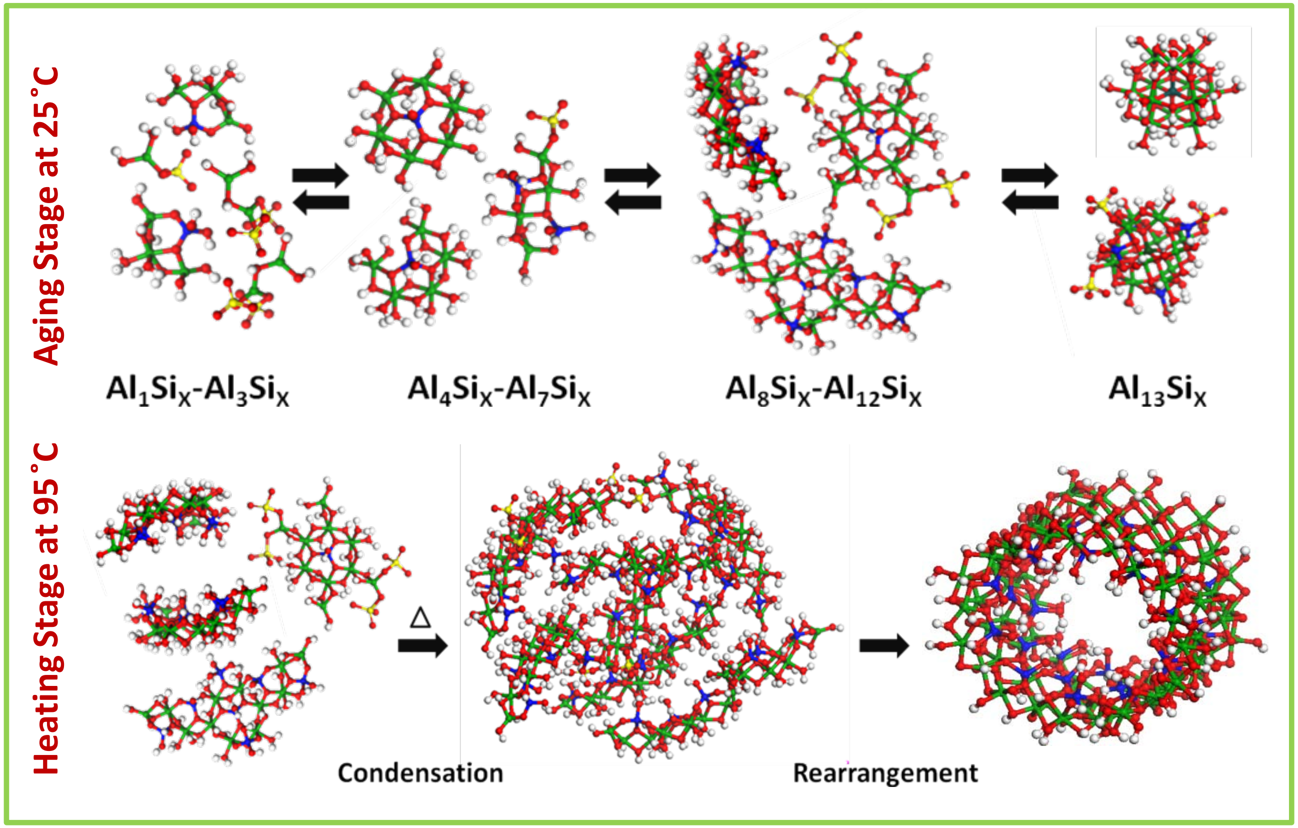

Yucelen, G. I., Choudhury, R. P., A. Vyalikh, A. Scheler, U, Beckham, H. W. and Nair, S. "Formation of Single-Walled Aluminosilicate Nanotubes from Molecular Precursors and Curved Nanoscale Intermediates", *Journal of the American Chemical Society*, 2011. 133(14): p. 5397-5412.

Shaping Single-Walled Metal Oxide Nanotubes

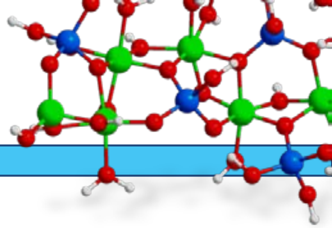

- Hypothesis – a relationship between the precursor shape and the resulting nanotube
- Can we achieve Ångstrom-level control over precursor and nanotube curvature?
- Binding of ligands such as perchlorate (ClO_4^-), chloride (Cl^-), and acetate (CH_3COO^-)

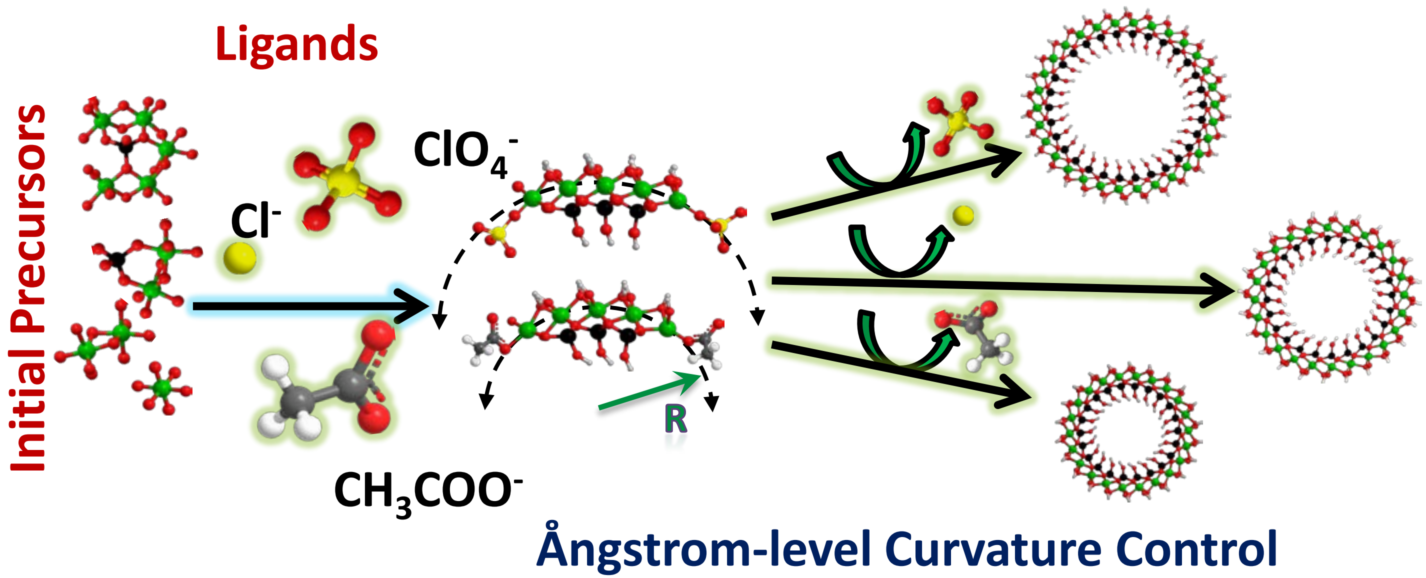

XRD, Nitrogen Physisorption, and NMR

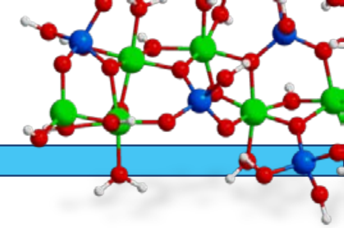

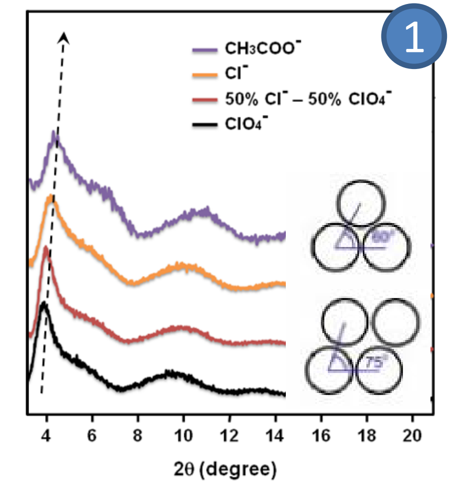

Experimental XRD patterns

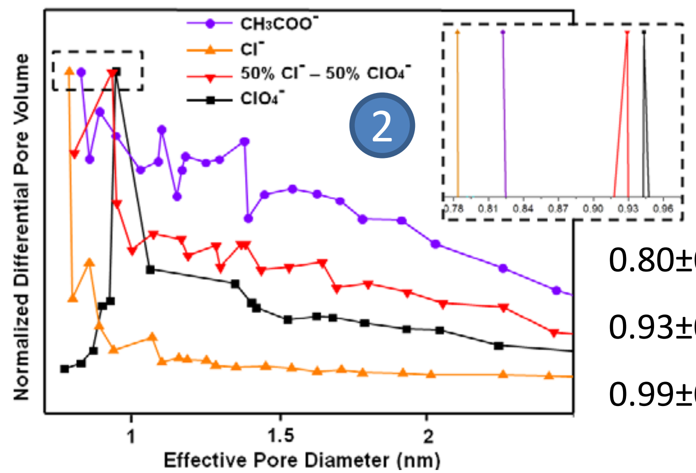

0.80±0.02 nm ⟶ 0.05 M HCl

0.93±0.05 nm ⟶ 0.05 M 50%HCl-50%$HClO_4$

0.99±0.06 nm ⟶ 0.05 M $HClO_4$

Pore Diameters – N_2 Physisorption Studies

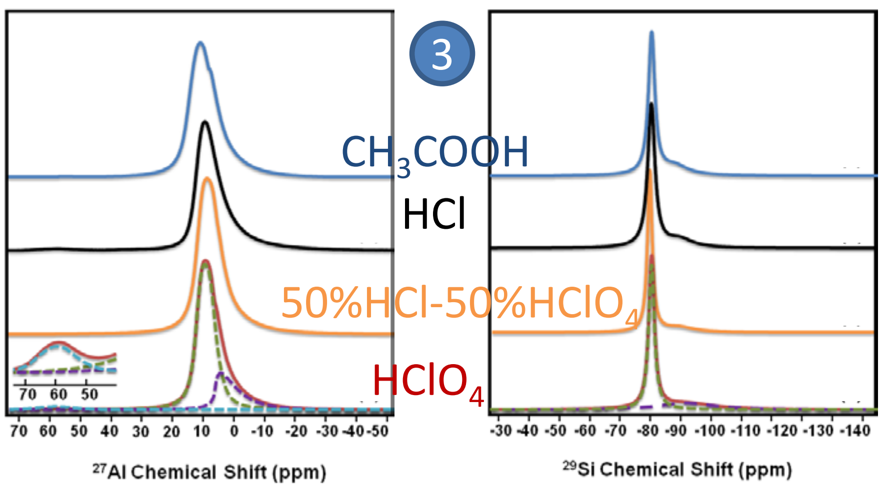

^{27}Al and ^{29}Si MAS NMR

- Experimental results support the hypothesis
- Largest external diameters obtained by ClO_4^-
- Nanotube composition is preserved

Cryo-Electron Microscopy

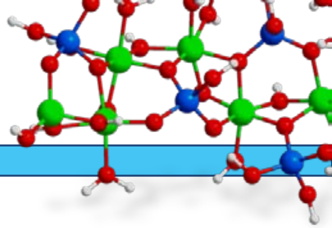

- Nanotube diameters are measured from high-resolution cryo-EM micrographs
- Nanotube diameter was determined based on measurement of 50 nanotubes
- Largest diameters obtained by the use of $HClO_4$, smallest by the use of CH_3COOH

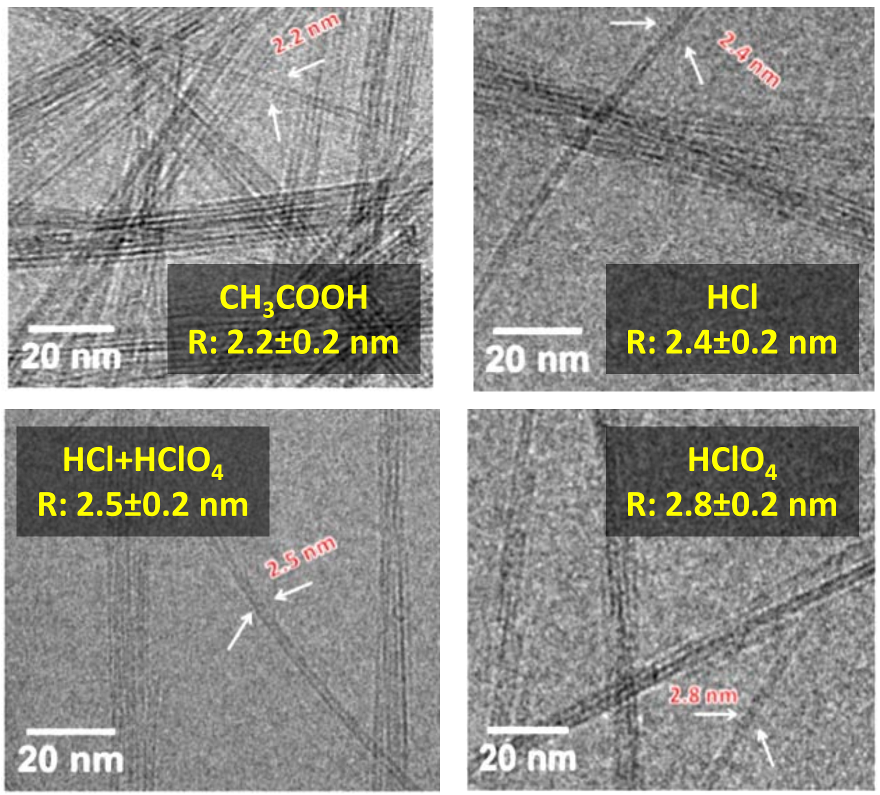

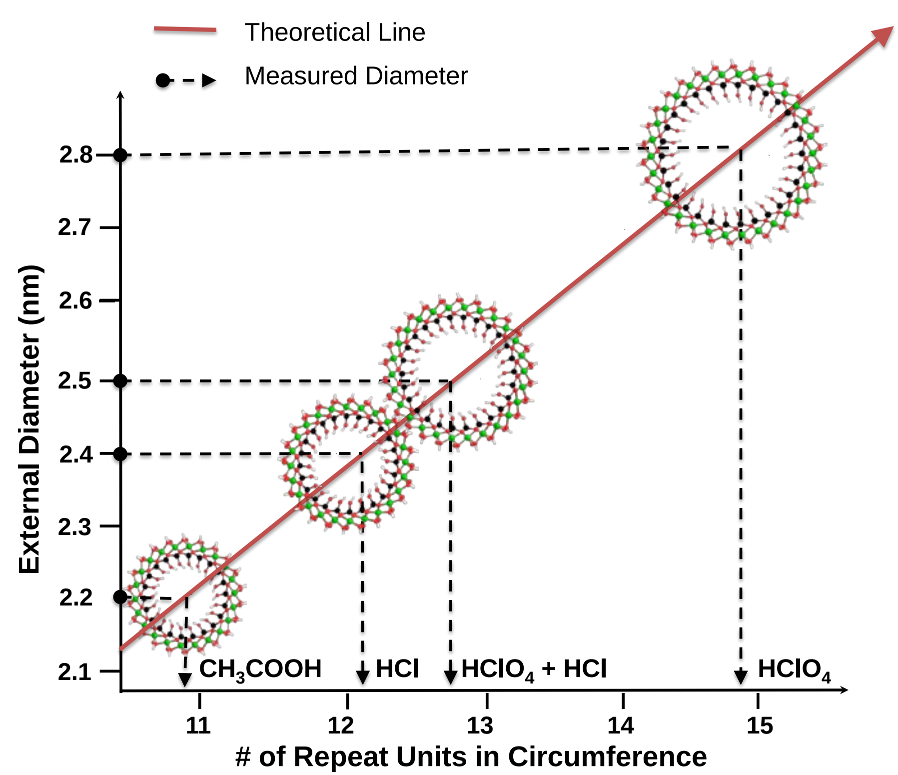

Ångstrom-level Diameter Control

Curvatures of DFT-optimized nanoscale intermediates

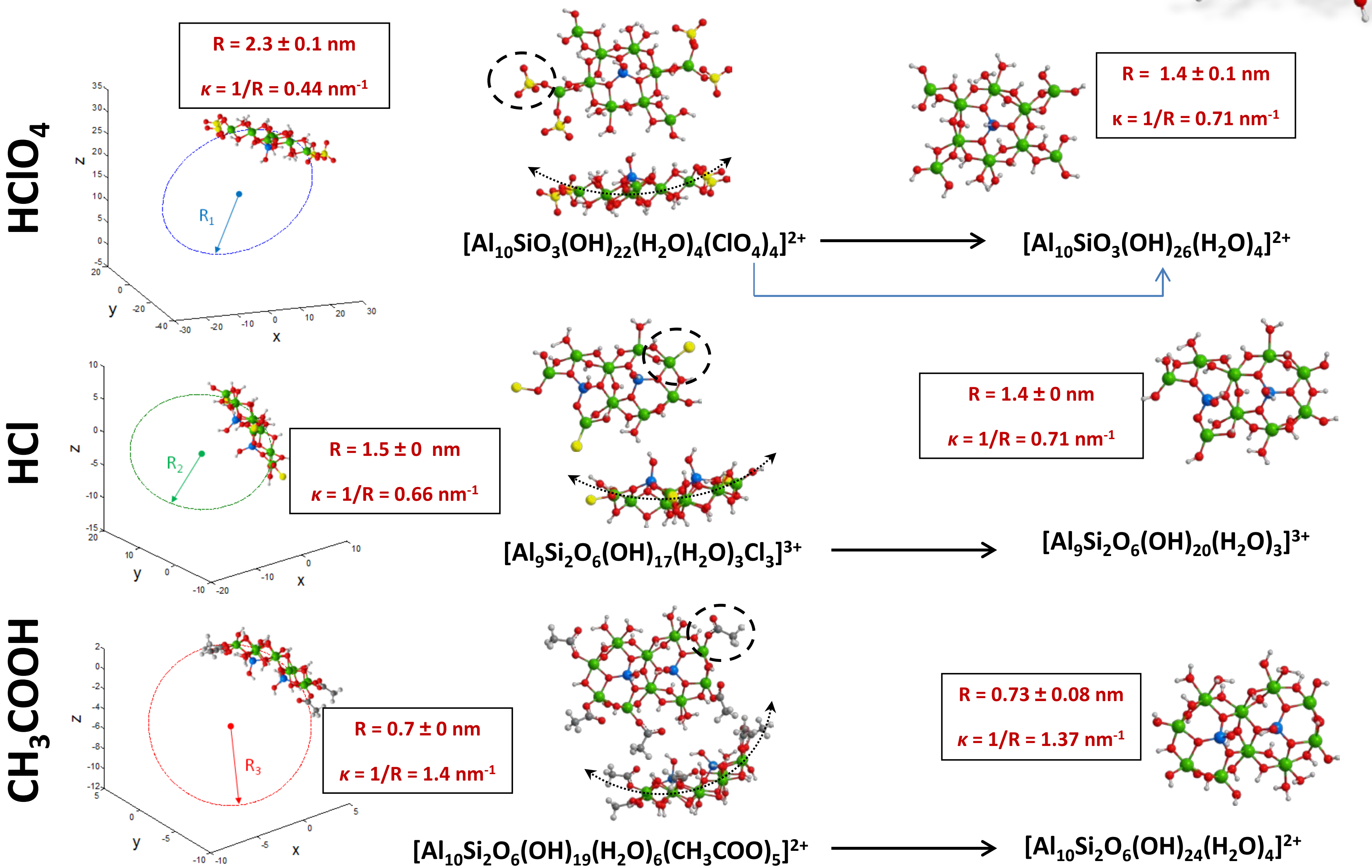

Shaping Single-Walled Metal Oxide Nanotubes

- There is a clear correlation between the precursor curvatures and the diameters of the nanotubes obtained.
- The **precursor curvatures** follow the trend of **$HClO_4$<HCl<CH_3COOH**, and the **nanotube diameters** correspondingly follow the inverse trend **$HClO_4$>HCl>CH_3COOH**

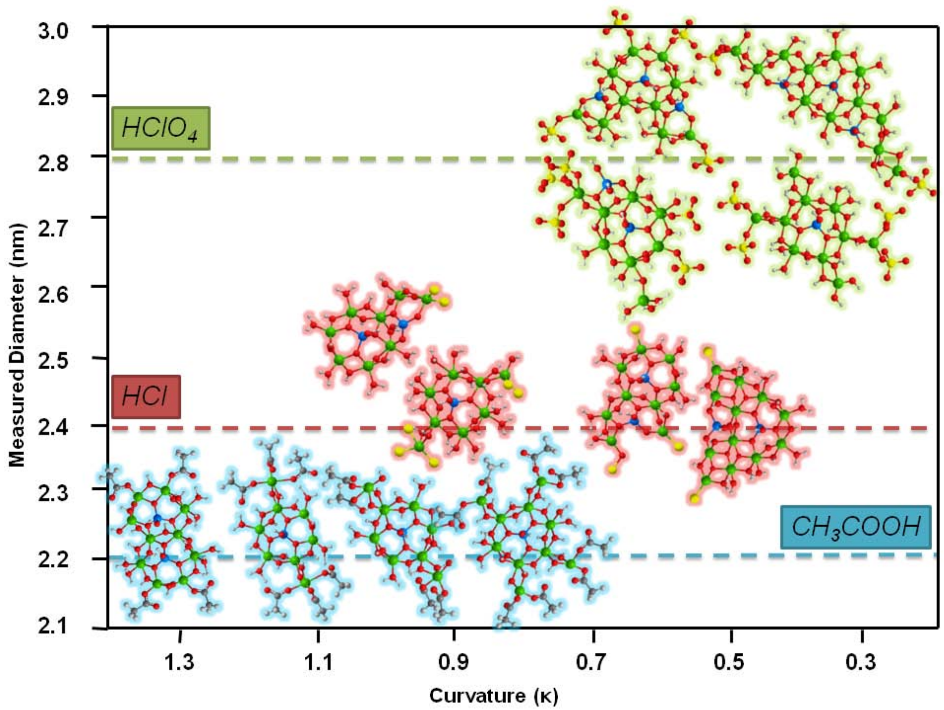

Yucelen, G.I., Kang, D-Y, Guerrero-Ferreira, R. C., Wright, E. R., Beckham, H. W. and Nair, S., "Shaping Single-Walled Metal Oxide Nanotubes from Precursors of Controlled Curvature", *Nano Letters*, 2012. 12(2): p. 827-832.

Modelling Nanotube Formation and Growth Mechanisms

Quantitative kinetic model formulation:

$$nP \xrightarrow{k_1} A \xrightarrow{k_2} NT_i \qquad (i = a,\ a = n/4)$$

$$NT_i + P \xrightarrow{k_3} NT_{i+1} \qquad (i \geq a,\ a+1,\ a+2, \ldots, N)$$

$$NT_i + NT_j \xrightarrow{k_4} NT_{i+j} \qquad (i, j \geq a,\ a+1,\ a+2, \ldots, N)$$

$$\frac{d[P]}{dt} = -nk_1[P]^m - k_3[P][NT]$$

$$\frac{d[A]}{dt} = k_1[P]^m - k_2[A]$$

$$\frac{d[NT]}{dt} = k_2[A] - k_4[NT]^2$$

$$\frac{d[NT]_i}{dt} = k_2[A] - k_3[P]NT_i - k_4 NT_i[NT] \qquad (i = a)$$

$$\frac{d[NT]_k}{dt} = k_3[P][NT_{k-1} - NT_k] + \frac{1}{2}k_4\left(\sum_{\substack{i=a \\ j=k-i}}^{i=k-1} NT_i NT_j - 2NT_k \sum_{i=a}^{N} NT_i\right) \qquad (k > a)$$

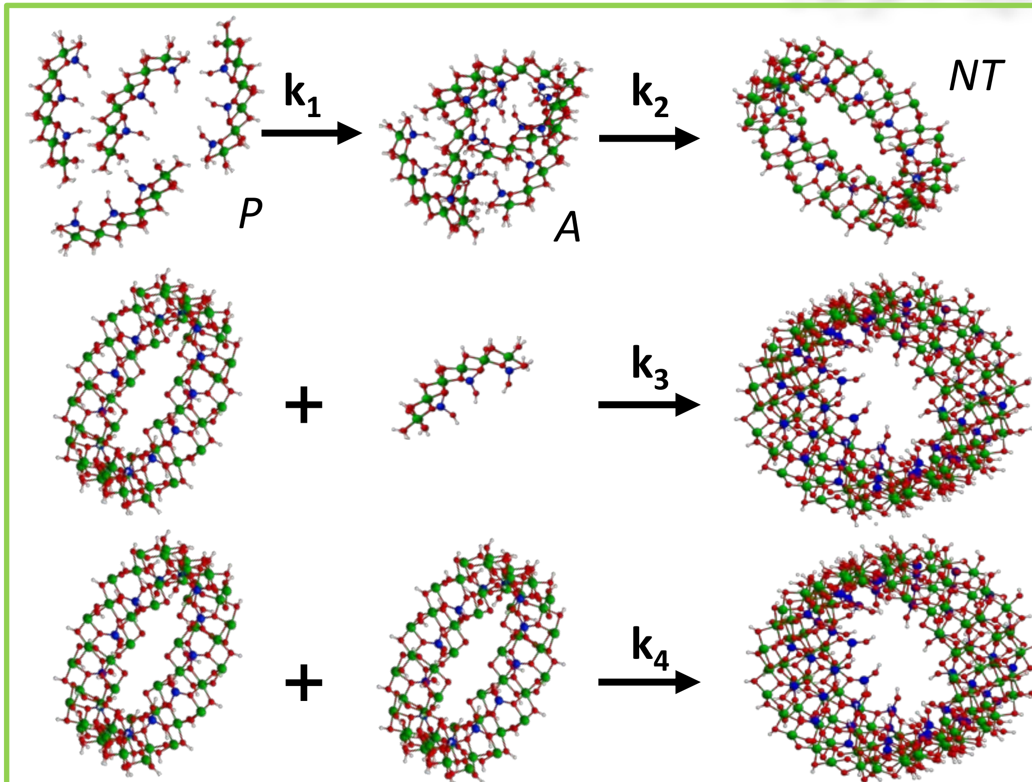

- Three primary type of species coexist in synthesis solutions: P, A, and NT
- Nanotube synthesis and growth is assumed to be a four-step process

Model Fitting and Validation

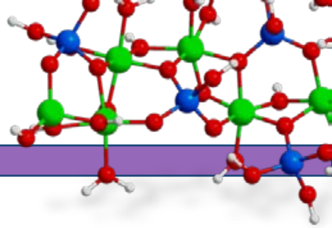

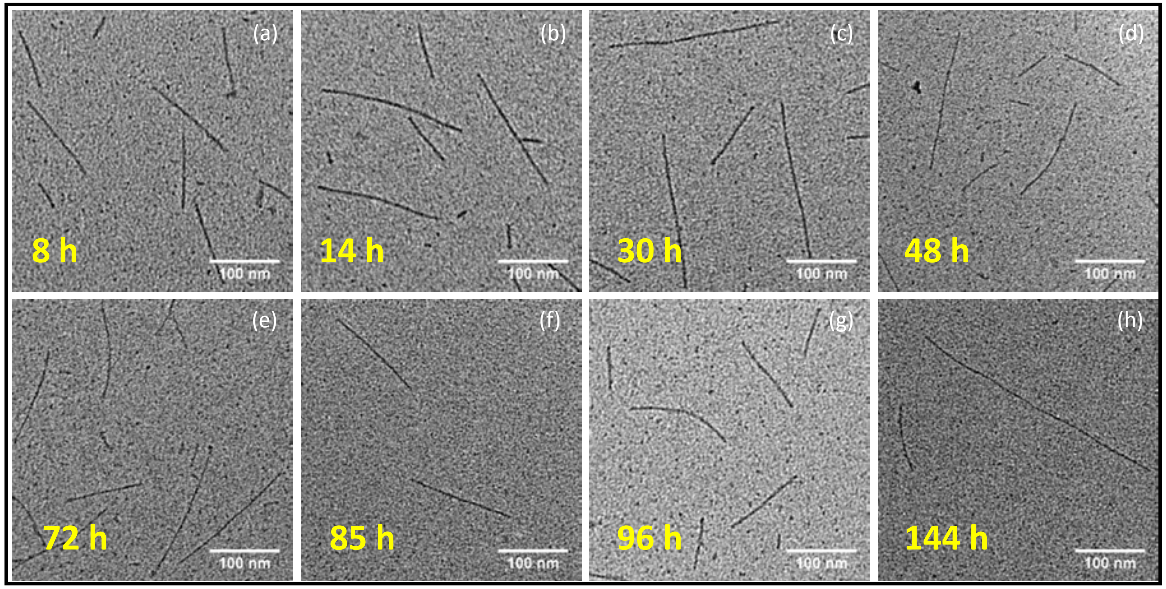

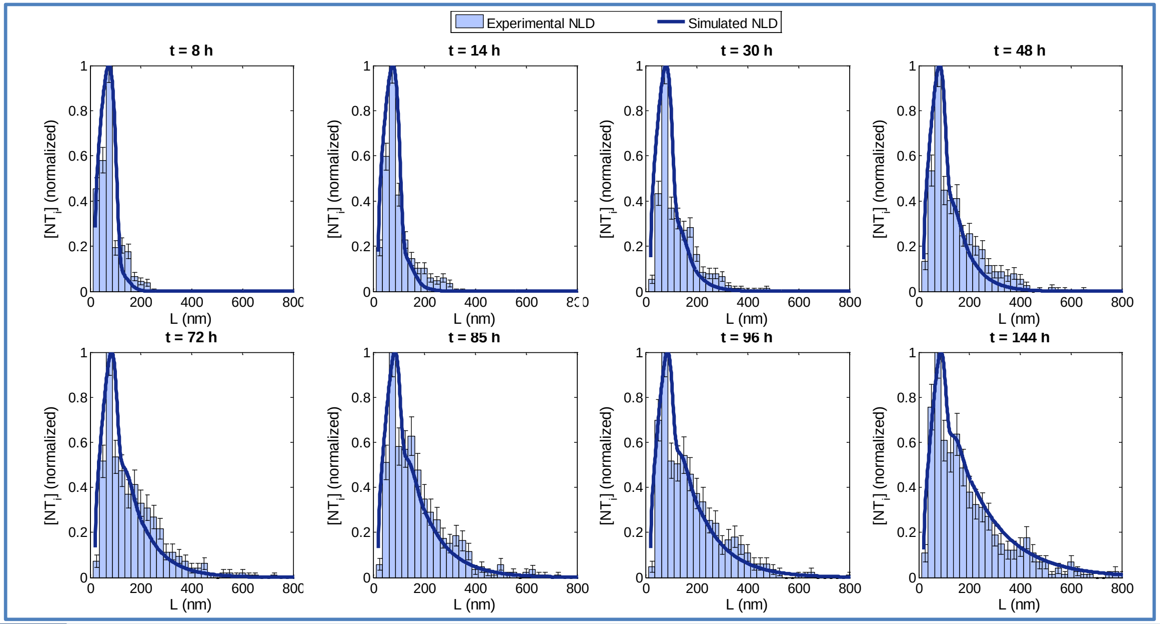

Reaction Constants	AlSiOH NT Synthesis
k_1 ($M^{-m}s^{-1}$)	1.4×10^{7}
k_2 (s^{-1})	2.2×10^{-4}
k_3 ($M^{-1}s^{-1}$)	2.8×10^{2}
k_4 ($M^{-1}s^{-1}$)	19.4
n	80
m	3.9
P_0 (M)	8.0×10^{-5}

- Dimensional evolution is studied by TEM
- Model captures all features of the NDLs (~10% avg. error)

Model Predictions

- The model is able to predict NLDs and mean lengths of nanotubes when P_0 is increased and decreased by 50 percent

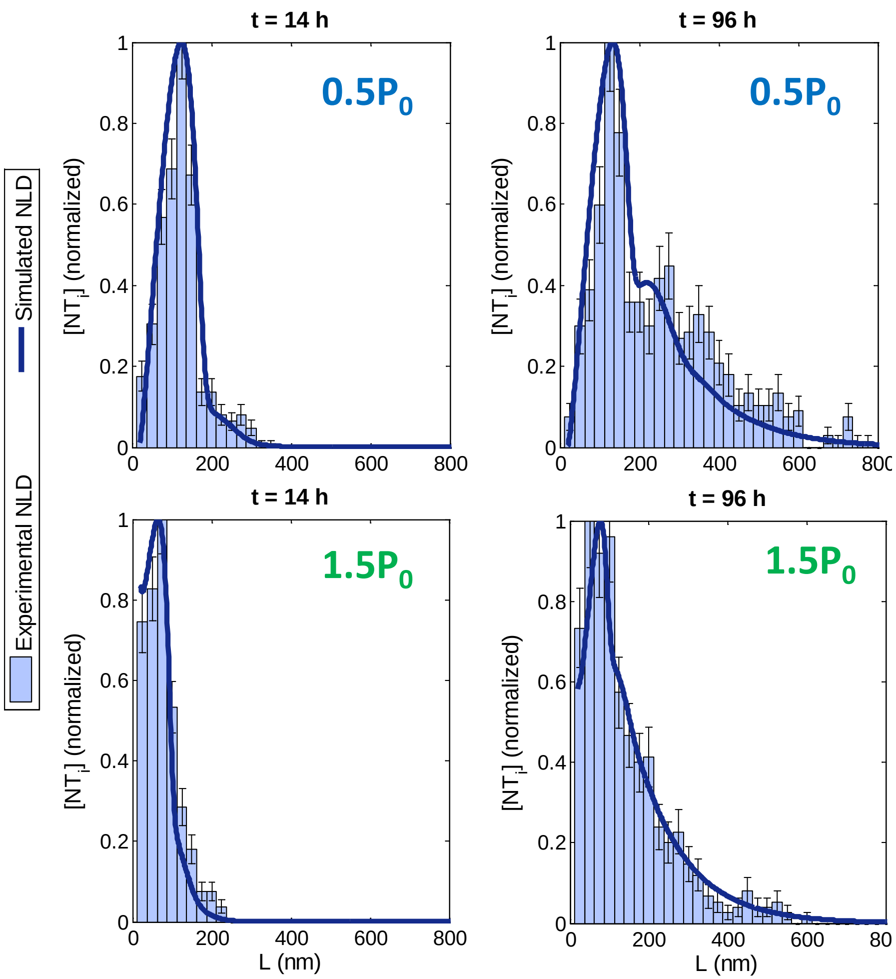

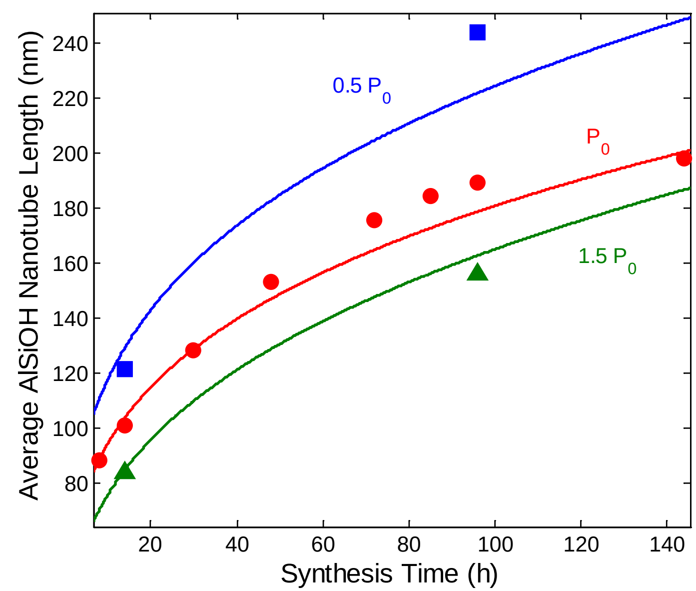

0.5P_0, t=96 h

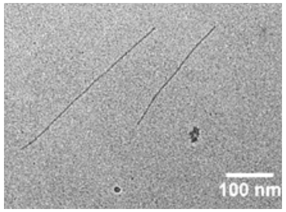

1.5P_0, t=96 h

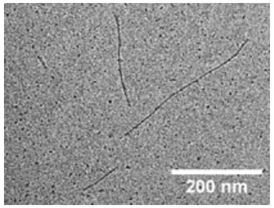

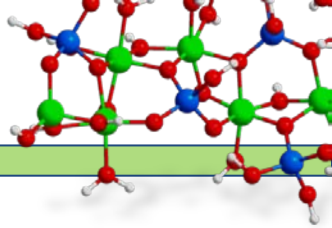

Thank You!!!

PORUS MATERIALS AND MEMBRANES *via*
NANOSCALE PROCESSING STRATEGIES

Nair Research Group

Beckham Research Group

ACKNOWLEDGMENTS:
This work was supported by The National Science Foundation (CAREER, CBET-0846586)

COLLABORATORS:
Prof. E. R. Wright (The Robert P. Apkarian Integrated Electron Microscopy Core of Emory University)
Prof. F. Fernandez (Chemistry & Biochemistry, Georgia Tech)
Dr. J. Leisen (Parker H. Petit Institute of Bioengineering and Biosciences, Georgia Tech)